Immune-Inspired Search Strategies for Robot Swarms

G. M. Fricke*[1], J. P. Hecker[1], J. L. Cannon[2,3], and M. E. Moses[1,4,5]

[1]*Department of Computer Science,* [2]*Department of Molecular Genetics and Microbiology,* [3]*Department of Pathology,* [4]*Department of Biology, The University of New Mexico, Albuquerque*
[5]*Santa Fe Institute, Santa Fe*

*mfricke@cs.unm.edu

May 24, 2016

Abstract

Detection of targets distributed randomly in space is a task common to both robotic and biological systems. Lévy search has previously been used to characterize T cell search in the immune system. We use a robot swarm to evaluate the effectiveness of a Lévy search strategy and map the relationship between search parameters and target configurations. We show that the fractal dimension of the Lévy search which optimizes search efficiency depends strongly on the distribution of targets but only weakly on the number of agents involved in search. Lévy search can therefore be tuned to the target configuration while also being scalable. Implementing search behaviors observed in T cells in a robot swarm provides an effective, adaptable, and scalable swarm robotic search strategy. Additionally, the adaptability and scalability of Lévy search may explain why Lévy-like movement has been observed in T cells in multiple immunological contexts.

1 Introduction

1.1 Search in Swarm Robotics

Robot swarms typically consist of many small, relatively simple and inexpensive robotic agents that work collectively toward some common goal (Brambilla et al., 2013). Swarm robotic algorithms are often inspired by biological systems that generate emergent collective behavior from the interactions of robots and their environment (Sahin, 2005). A major research challenge is the development of swarm robotic algorithms that allow effective navigation through complex real-world environments without centralized control (Winfield et al., 2005; Hecker and Moses, 2015).

Foraging is a canonical problem in swarm robotics in which robots have to locate targets distributed in space and transport those targets to some specified location (Winfield et al., 2005). Hecker and Moses (2015) demonstrate an ant-inspired algorithm, Central-Place Foraging Algorithm (CPFA), that is error tolerant, adaptable to different resource distributions, and scalable across swarm sizes. The CPFA uses parameters selected by a Genetic Algorithm (GA) to govern correlated random walks and the use of shared information. Here, we present an immune-inspired search pattern that can be adapted to replace the more complex search behavior used in the CPFA. An advantage of a simpler pattern is that it can be more easily analyzed and tuned for maximum search performance given different resource distributions and swarm sizes. The search pattern discussed in this work is simple, efficiently scales with the number of searchers, is robust to error, is adaptable to the distribution of targets, and requires no centralized control.

As robots have become smaller, cheaper, and are increasingly expected to operate in natural environments, designing flexible and error tolerant algorithms for robot swarms has become more important. Robots swarms are often constructed with cheaper

components than monolithic robots, which increases the chance of component failure and decreases the accuracy of actuation and sensor input. The small size of swarm robots and their operation in natural environments can also lead to robot loss. Therefore, it is advantageous for swarms to be resilient to individual robot loss and to the effects of sensor error.

Robustness is the ability to cope with the loss or malfunction of individuals. Malfunction may result in loss of agents or in soft errors, such as failure to detect a target due to imperfect sensors. Robustness can be improved by redundancy and decentralized control that avoid single points of failure. *Scalability* is the ability to perform well with different group sizes. Search strategies that can be tuned to optimize performance for different target configurations are *adaptable*.

The success of robot swarms searching for targets in an unknown environment depends on the adaptability and robustness of the search strategy. Such tasks include surveying planetary surfaces (Fink et al. (2005), Stolleis et al. (2016a,b) in press), land and sea mine clearance (Weber, 1995), pollution mapping by subsurface robots (Hu et al., 2011), agriculture (Tamura and Naruse, 2014), survivor location in hazardous environments (Birk and Carpin, 2006) as well as military applications (Love et al., 2015).

Sensor and actuation error are crucial motivation for using a stochastic search strategy. Though most robot swarms remain confined to simulation (Brambilla et al., 2013), error models should be derived from an embodied physical system. We use a previously published simulation of inexpensive, ant-inspired iAnt robots that are capable of movement, memory, and communication (Hecker and Moses, 2015). We extend the simulation in order to scale our immune-inspired search pattern to 32 robots. The simulation was written in tandem with development of the physical robots and approximates the performance and sensing and navigation error of real iAnts (Hecker et al., 2013).

Our use of a stochastic search strategy is in part motivated by Ackley et al. (2012). Computational processes that guarantee correctness are no longer tenable as systems increase in size and complexity; rather, large distributed systems should sacrifice determinism for robustness. This recent recognition of the value of robustness builds on earlier work by Von Neumann (1951), which recognized that if computing systems were ever to become truly scalable, they would need to take on aspects of biological systems that are both robust to the failure of individual parts and inherently stochastic.

1.2 Search in Immunology

T cell search patterns in the immune system are robust, efficient, adaptable, and scalable. T cells search collectively but without centralized control (Groom et al., 2012; Sung et al., 2012; Textor et al., 2014). In order to initiate the adaptive immune response, T cells search for dendritic cells in lymph nodes (Figure 1). Receptors on the T cell surface bind to antigen indicative of infection that are presented on the surface of dendritic cells. This search process is analogous to a swarm of robots searching for targets.

Detecting and destroying pathogens early during an infection, before they become unmanageable, relies on minimizing the time taken for T cells to detect pathogens. Efficient search is crucial to mounting a timely and effective immune response against pathogen populations that often expand geometrically (Mirsky et al., 2011).

Immune system search must also scale efficiently with the number of T cells. When an immune response is triggered, activated T cells proliferate geometrically (De Boer et al., 2001); increasing, in a matter of days, from a population on the order of 10 cells to millions. Just as robots may be lost or malfunction, T cells may die or malfunction, changing the number of searchers during the course of a search.

T cell search is robust to error in the antigen detection process. Each T cell bears receptors capable of being activated by a specific set of antigens. T cell receptors sense their local environment through direct contact with antigen, an inherently noisy and stochastic sampling process. T cell detection of target antigen is susceptible to false negatives especially when antigen is in low concentrations (Fricke and Thomas, 2006).

(a) (b)

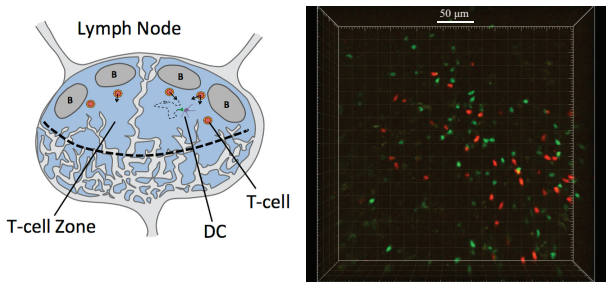

(c)

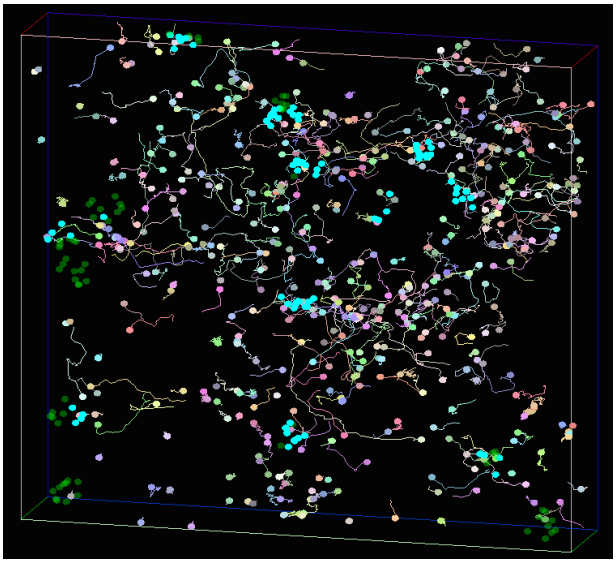

Figure 1: T cell movement in a mouse lymph node. (a) Schematic diagram of a lymph node in which T cells search for dendritic cells (DCs) (Fricke et al., 2013). (b) Two-photon image of T cell zone with T cells fluorescing in red and green. (c) Model of T cell movement with dendritic cell targets in green and T cell tracks in various colors (Fricke et al., 2016).

T cell search strategies should also be adaptable to different target configurations. Pathogens exhibit an array of growth strategies and patterns (Lindquist et al., 2004; Miller et al., 2004) that result in a variety of antigen distributions and concentrations. The tissues through which T cells search also influence the distribution of pathogens. For example, T cells search an essentially 2-dimensional space in the epithelium (Ariotti et al., 2012), while T cells in the lungs and brain must navigate higher dimensional search spaces (Harris et al., 2012).

Effective T cell search within the lymph node environment is particularly important because it initiates the adaptive immune response. In lymph nodes naïve T cells search the T cell zone for dendritic cells carrying cognate antigen brought from peripheral tissue (Figure 1a). The volume of the T cell zone is on the order of 10^6 times that of a T cell. Interaction of T cells with dendritic cells presenting cognate antigen leads to T cell activation. Once activated T cells replicate, migrate out of the lymph node, and search for antigen in peripheral tissues such as brain and lung.

The requirements for search by robot swarms are similar to those encountered by T cells in search of pathogens. An effective immune response requires T cells to minimize the time taken to find antigen distributed in a wide variety of spatial configurations using swarm sizes that vary by orders of magnitude, and with imperfect target detection. We apply an observed T cell stochastic search strategy to a robot swarm with noisy sensors and explore the scalability, adaptability, and efficiency of that search.

1.3 Lévy Search

Searching for targets, when there is insufficient time to explore the entire search space necessarily involves a trade-off between search *intensity* and search *extent* (Méndez et al., 2013). Search extent is a measure of how far the searcher travels from the starting location, while intensity is a measure of local search thoroughness. The optimal trade-off depends on the distribution of targets. We find that Lévy search patterns can be tuned to easily and effectively manage this trade-off.

Lévy search consists of step lengths that fit a power law distribution, where *step length* is defined to be the displacement (shortest distance) between consecutive positions. Most step lengths are small, but with a heavy-tail, that is, a decreasing probability of larger steps and a non-zero probability of steps of any length. In a Lévy search pattern, the

direction of search at each step is drawn from a uniform distribution and is independent of previous steps (i.e. is isotropic and Markovian) (Mandelbrot, 1983; Viswanathan et al., 1996). We, and others, find Lévy search to be a useful mathematical abstraction of these patterns of motion, while noting that Lévy search does not capture the complexity of T cell movement. T cell motility is an active area of research for which multiple models of search have been proposed, for example, in peripheral tissues (Potdar et al., 2008) and in lymph nodes (Banerjee et al., 2011; Donovan and Lythe, 2012; Gérard et al., 2014; Banigan et al., 2015). T cell movement in the brain has displacement consistent with a Lévy search (Harris et al., 2012), and T cells in lymph nodes have a heavy-tailed distribution of step lengths (Fricke et al., 2016).

Lévy search patterns are stochastic fractals. The Probability Density Function (PDF) that governs the distribution of step lengths used to generate a particular Lévy pattern is a power law:

$$\mathrm{L}(x) \propto x^{-\mu} \tag{1}$$

where $\mathrm{L}(x)$ is the probability of a searcher moving in a straight line for distance x. The exponent μ that determines the shape of the PDF is known as the Lévy exponent.

Stochastic search has been studied extensively by biologists, especially mathematical ecologists. Ecologists typically state the problem of efficiency in the interaction of searchers and targets as one of foragers and food items. Foraging problems and immunological search have much in common.

The Lévy foraging hypothesis was first developed in order to explain the disparity between observed super-diffusive animal motion and Brownian random walk models. Animals searching for food tend to maintain relatively straight trajectories for longer distances than would be produced by a Brownian searcher. Lévy search has been used to explain the foraging patterns of numerous species including reindeer (Mårell et al., 2002), albatross (Viswanathan et al., 1996), and human foragers (Raichlen et al., 2014). James et al. (2011) provide a more comprehensive list along with a criticism of Lévy search analysis.

Whether these search patterns are truly power law distributed is a matter of ongoing debate (Bartumeus et al., 2005; Edwards, 2011; Humphries et al., 2012). The issue is clouded in part because a true power law distribution of step lengths is impossible in a finite space. The question then is whether animals or cells use a truncated power law distribution of step lengths constrained by the environment in which they are searching.

In this work we examine the properties of Lévy search patterns because they provide a model of search that captures aspects of the heavy-tailed movement patterns observed in T cells, are simple enough to be translated into robots, and exhibit the properties of robustness, scalability, and adaptability that are required of T cells and robot swarms.

We explore the relationship between target configurations, the number of robot searchers, and μ in Equation (1), where μ is selected by a GA. We confine our robots to a $100\,\mathrm{m}^2$ arena, which places an upper limit on the distance searchers can travel without turning. Similarly, since power laws diverge as step lengths approach zero, we define a minimum step length for our robots to be 8 cm. Even with these constraints we show that the mathematical properties of Lévy search can be used to engineer a search pattern for robots with desirable properties.

2 Related Work

2.1 Robotic Lévy Search

In work related to our own, Van Dartel et al. (2004) evolve neural controllers for agents searching a simulated world with targets drawn from a uniform distribution. The authors observed convergence of the best performing robots to a Lévy search pattern defined by a power law PDF exponent of 2 ($\mu = 2$ in Equation (1)), consistent with optimal foraging behavior described by Viswanathan et al. (1999).

Swarm robot simulations have used Lévy search in combination with chemotaxis-inspired gradient sensing (Nurzaman et al., 2009) and artificial potential fields (Sutantyo et al., 2010) to efficiently search unmapped spaces with range-limited sensors. The au-

thors of these papers fix the Lévy exponent to 2, and explore a uniformly random distribution of targets.

Sutantyo et al. (2010) report that when collisions increase significantly with the number of searchers, performance scales sub-linearly. The rate of collision between searchers is determined by a number of factors, including the effectiveness and cost of collision avoidance algorithms and the size of searchers relative to the rate of displacement. Hecker and Moses (2015) find that even when collisions are ignored, efficiency does not scale linearly with the number of robots. Our simulation similarly ignores collisions, allowing us to isolate the effect of oversampling on search performance.

Sutantyo et al. (2013) incorporate Lévy search into a firefly optimization algorithm for an underwater robot swarm consisting of 5 robots. They examine two target distributions: sparse and clustered. They find that Lévy search with $\mu = 2$ outperforms two alternate stochastic search strategies.

Keeter et al. (2012) use underactuated robots implementing Lévy search in a 3D aquatic environment to locate four uniformly distributed targets. They sample various values of μ in 0.5 increments in the range $1.1 < \mu < 3$ and report a monotonic improvement in search time as μ approaches their lower bound of 1.1.

In order to measure the ability of Lévy search to explore an environment with barriers, Katada et al. (2015) use 3 robot swarms of different sizes to solve a search problem inside a building with occluding walls. The robots are required to maintain a line-of-sight connected communication network while searching for a single cluster of targets. The effectiveness of a Lévy search with fixed $\mu = 1.2$ is compared to Brownian search and found to reduce search time.

In the work above, either the Lévy exponent, the number of robots, or the distribution of targets is fixed. Here we systematically map the relationship between Lévy exponents selected by a GA and a variety of swarm sizes and target configurations. This allows us to determine whether and how the optimal Lévy exponent depends on target configuration and swarm size.

Beal (2015) examines the effectiveness of Lévy search as a mechanism for positioning robots such that they provide even coverage of a given area with obstacles. Beal identifies a trade-off between *aggressiveness* and *evenness* in the pattern of dispersal. These concepts have interesting connections to the ideas of intensity and extent in our own work. However, their formulation of the coverage problem is significantly different from our work (the lack of discrete targets, for example) and does not address search performance.

2.2 Lévy Search with Heterogeneous Target Configurations

Nurzaman et al. (2011) describe an E. coli inspired correlated random search that is similar to the search strategy described in Hecker and Moses (2015). In this model turning angle correlation is proportional to target density. The resulting pattern of motion is fit to a power law and the Lévy exponent, μ, estimated. The best-fit mean value of μ decreases from 3.03 to 2.2 as target density is reduced.

Raposo et al. (2011) model the relationship between heterogeneity of searcher target distance and optimal μ values. Using a 1-dimensional analysis they predict that decreasing μ will increase the success of target encounters in heterogeneous landscapes. They suggest that this theoretical result generalizes to the 2-dimensional case. However, they do not test this hypothesis as we do here.

2.3 Lévy Search in Immunology

Harris et al. (2012) examined T cell search patterns in the brains of *Toxoplasma gondii* infected animals. They found the pattern of motion to be superdiffusive, and consistent with a generalized Lévy search with $\mathrm{L}(x) \propto x^{2.15}$, $\mu = 2.15$ in Equation (1). In supplemental material the authors also describe a computer simulation of Brownian motion and the generalized Lévy search in a sphere. Harris et al. (2012) report that the Lévy search was able to detect targets an order of magnitude more efficiently than Brownian motion. In our own work, we also find an order of magnitude decrease in first contact times when using a Lévy vs. Brownian search (Fricke et al., 2013).

We investigated the movement patterns of T cells searching for dendritic cells in lymph nodes and find that they balance the extent and intensity of search (Fricke et al., 2016). The difference between Lévy search and Brownian search decreases, though is still significant, when the efficiency metric is normalized by the total distance searchers cover. T cells use strategies that have aspects of Lévy search, but Lévy search by itself is unable to explain the full range of search behavior. This is not surprising given that immunological search is the result of extremely complex interactions between numerous cell types communicating via a range of chemical signals. Despite this, we find the Lévy foraging hypothesis (Viswanathan et al., 1999) to be a useful model of T cell search in peripheral tissue (i.e. the brain (Harris et al., 2012)) and in lymph nodes. In addition, Lévy search patterns provide a effective engineering approach for designing searchers with desirable properties.

3 Stochastic Fractal Search

Deterministic search strategies may be effective in relatively fixed environments and when localization is error free. Theoretically, systematic raster scan search outperforms stochastic search (Bénichou et al., 2011; Keeter et al., 2012). However, in environments where target configurations are unknown or change over time, stochastic search strategies are more effective (Stephens and Krebs, 1986; Acar et al., 2003). Deterministic strategies depend on accurate information about the searchers' current location, and the ability to move from the current location to the next without error, which is difficult in practice even with global positioning systems (Humphreys et al., 2008; United States Department of Defense, 2008; Maier and Kleiner, 2010).

Errors in sensor input and in actuation introduce randomness into even apparently deterministic processes. iAnt robots are underactuated (i.e. are unable to follow arbitrary trajectories), and therefore the problem of error free navigation from one point to another is especially difficult. In contrast T cell motility mechanisms are holonomic with motion governed by cytoplasmic flow into membrane protrusions and an actin cytoskeleton that can be rapidly reoriented in any direction. T cell motion is stochastic, which may be due to environmental or intrinsic factors (Linderman et al., 2010; Celli et al., 2012; Harris et al., 2012; Textor et al., 2014). Like many swarm robots, T cells' sensors are short range, because they are limited to molecular interactions at the cell surface (Alberts et al., 2002).

Lévy search is easily related to the Hausdorff Fractal Dimension ($\mathcal{H}$), which provides a compact measure of the trade-off between intensity and extent. Increasing extent, by decreasing $\mathcal{H}$, results in increased displacement of searchers from their start positions as a function of time.

The fractal dimension of a search pattern is a measure of the fraction of locations visited in a search space. For example, Brownian motion has fractal dimension $\mathcal{H} = 2$, meaning that, asymptotically, a Brownian search pattern visits all positions in a 2-dimensional space.

When locations visited by a searcher consist of a sequence of disconnected points, the motion is called a Lévy flight (the searcher is flying or jumping from point to point). Since we consider space between points to be part of the area searched, our Lévy search is actually a Lévy walk (Shlesinger and Klafter, 1986).

As far as we are aware, the fractal dimension of Lévy walks has not been formalized, therefore we calculate $\mathcal{H}$ for Lévy flights. Since Lévy flights visit only end points of steps, $\mathcal{H}$ is the dimension of the visited point-set (Seshadri and West, 1982; Mandelbrot, 1983). $\mathcal{H}$ for Lévy walks will be strictly greater than that for Lévy flights. We hope to investigate the $\mathcal{H}$ of Lévy walks in future work.

The PDF governing Lévy search as formulated in Equation (2) not only describes the probability, $\mathrm{L}(x)$, of observing a step length of x, but also relates the resulting stochastic fractal to $\mathcal{H}$:

$$\mathrm{L}(x) = \frac{\gamma}{x_{\min}} \left(\frac{x}{x_{\min}} \right)^{-1-\gamma} \tag{2}$$

where, x is the step length, $x_{\min}$ is the smallest possible step length, and γ determines the decay rate of the step length probability distribution. $\mathcal{H} = \gamma$ in Equation (2) (Mandelbrot, 1983; Hughes, 1996). The

coefficient $\frac{\gamma}{x_{\min}}$ normalizes the area under the curve to be 1 so that Equation (2) is a PDF. Since $x_{\min}$ is a constant, and labeling the exponent μ results in Equation (1) so that,

$$\mathcal{H} = \mu - 1 \tag{3}$$

Brownian motion has $\mathcal{H} = 2$ (Taylor, 1961) and $\mu = 3$. The resulting walk is maximally intense when embedded in a 2-dimensional space.

The Mean Squared Displacement (MSD), a measure of search extent, of a population of searchers is also characterized by a power law:

$$\text{MSD} = \left\langle (\vec{r}(t + \Delta t) - \vec{r}(t))^2 \right\rangle \propto t^{\alpha} \tag{4}$$

where $\vec{r}(t)$ is the position vector of an agent at time t and $\vec{r}(t + \Delta t)$ is the location of an agent after some time increment Δt. The difference between $\vec{r}(t)$ and $\vec{r}(t + \Delta t)$ is the displacement between searcher positions at t and $t + \Delta t$. Angle brackets indicate the ensemble average over the population of searchers. The MSD exponent α describes the rate of displacement over time and is related to $\mathcal{H}$. As α increases, search extent increases.

The search patterns produced by a Lévy exponent, μ, between 1 and 3 are more extensive than Brownian motion but have lower $\mathcal{H}$ and so are less intensive. As μ approaches the limiting value of 1, the MSD and extent of search become infinite.

Figure 2 shows two search patterns. In panel (a) $\mu = 3$ resulting in panel (b), a Brownian pattern of search with diffusive motion ($\mathcal{H} = 2$ and $\alpha = 1$). The displacement of a Brownian random walk grows as the square root of time. Panel (c) shows a power law distribution resulting in Lévy search with $\mathcal{H} = 0.5$, and a superdiffusive pattern of motion with $\alpha > 1$.

MSD describes how far searchers are likely to travel from their starting locations over time. The fractal dimension determines how thoroughly an area is searched. Both MSD and the fractal dimension are governed by a single parameter μ. Changing μ allows control over the extent and intensity of search, a property we exploit in order to adapt the robot swarm to the distribution of targets.

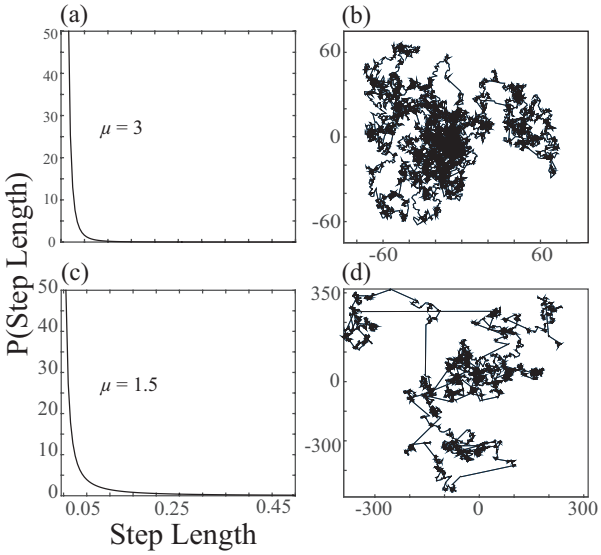

Figure 2: Stochastic fractal search patterns resulting from uniform turning angles with a power law distribution of step lengths. (a) Power law exponent $\mu = 3$, fractal dimension ($\mathcal{H}$) = 2, and Mean Squared Displacement (MSD) exponent $\alpha = 1$, and (b) a resulting thorough Brownian pattern of search visualized in the plane. (c) $\mu = 1.5$, $\mathcal{H} = 0.5$, $\alpha > 1$, and (d) a resulting Lévy search with lower dimensionality and greater extent.

4 Methods

4.1 iAnt Robot Platform

iAnts are small autonomous robots that move with constant speed and use an onboard iPod for computation and sensors (Figure 3a). The iAnt simulator replicates the movement and sensing capabilities of iAnts (Figure 3b).

The CPFA performed by an iAnt swarm has several phases, including a stochastic search phase implemented as an adaptive correlated random walk. Here, we implement the Lévy search as an alternative stochastic search strategy. The parameters for this search are determined by a GA which evolves simulated iAnt parameters and produces a strategy for the physical robots to use in the search task.

(a)

(b)

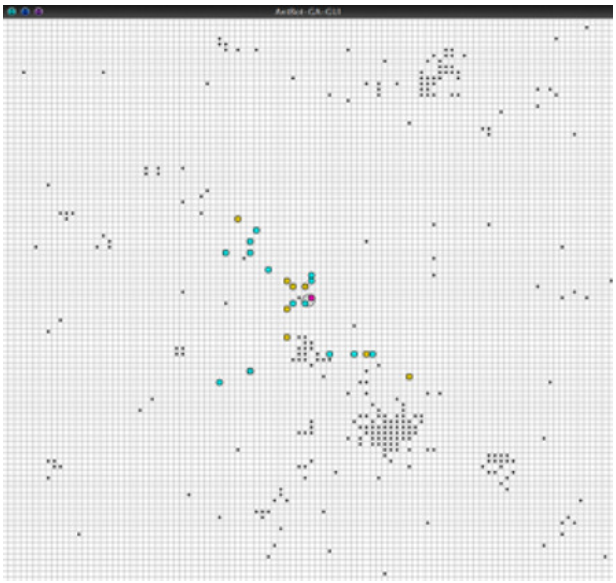

Figure 3: The iAnt Robot System. (a) Robots searching for targets. The targets are QR tags attached to poker chips. The lamp corresponds to the robot start position. (b) Simulation of the physical iAnt robots in a 100 m^2 search arena. Grey dots are targets. Colored circles are robots: red is at the start position, green are searching robots, blue are robots that found a target. The simulation incorporates error modeled from the physical iAnts.

Hecker et al. (2013) observed that iAnt robots fail to observe targets within their viewing range 43% of the time. We incorporate this error in our simulations.

4.2 Robot Lévy Search

Lévy search is defined by the $\mathcal{H}$ of the random path they generate. In order to analyze the relationship between Lévy search efficiency and the distribution of targets, we have the iAnts generate a Lévy search with parameter μ (Equation (1)) and corresponding $\mathcal{H}$ (Equation (3)).

The GA explores the fitness landscape and optimizes μ to produce a search pattern with $\mathcal{H}$ that most efficiently solves the problem of detecting a particular distribution of targets.

iAnts draw a random variate, t, from a power law PDF (with units 0.5 s):

$$t = t_{\min}(\mathcal{U}(0,1))^{\frac{-1}{\mu-1}} \tag{5}$$

where $t_{\min}$ is the minimum time (0.5 s) and μ is evolved by the GA to maximize the discovery of targets. The GA is described in more detail in Section 4.4.

Each robot chooses a direction from a uniform distribution and moves in that direction for t time steps. At the end of this movement, a new t is drawn and the process repeats. Collisions with the edge of the search area require that the robot draw a new direction. In our experiments targets are discovered without replacement, resulting in a dynamic search landscape in which the density and spatial distribution of targets changes over time.

4.3 Cluster Analysis

We explore the optimized $\mathcal{H}$ evolved by the GA in response to various target configurations. To accomplish this we use 256 targets in every simulation but distribute them in varying numbers of clusters. For generality we measure the patchiness (distance from uniformly random) of the distribution of targets using the Hopkins index (Jain and Dubes, 1988).

We calculate $\mathcal{H}$ across varying numbers of clusters in order to characterize possible target distributions.

At one extreme all targets are in a single pile, and at the other all targets are uniformly distributed into 256 piles of one target each. We use two cluster progressions to map the Hopkins index to different configurations of targets: clusters with a linear progression, 1, 10, 20, ..., 100, and a power law progression, 1, 2, 4, ..., 256. Cluster centers are positioned by drawing x- and y-coordinates from a uniform PDF.

The Hopkins statistic tests spatial randomness by comparing nearest-neighbor distances from uniformly distributed points and randomly chosen targets. If there are n targets in the set T, then let $m \ll n$ and choose m sampling points $\mathrm{S} = \{s | s = (x, y)\}$, where x and y are chosen uniformly to be within the search arena. We randomly choose m targets, $\tilde{t} \subset \mathrm{T}$, to compare with S. If we define U and W to be,

$$\mathrm{U} = \sum_{j=1}^{m} ||s_j - t||, \forall t \in \mathrm{T} \qquad \mathrm{W} = \sum_{k=1}^{m} ||\tilde{t}_k - t||, \forall t \in \mathrm{T} \tag{6}$$

Then the normalized Hopkins index is,

$$\mathrm{H} = \frac{\mathrm{U}}{\mathrm{U} + \mathrm{W}} \tag{7}$$

Intuitively, the Hopkins index compares (as a normalized ratio) W, the distribution of distances between targets, and U, the distribution of distances between targets and a set of uniformly distributed points. The resulting ratio is a dimensionless statistic that does not depend on the units used to measure distance. The values of the Hopkins index lie in the interval $[0.5, 1]$. For uniformly random point locations, the expected value is 0.5. As targets become more highly clustered, the value of the Hopkins index approaches 1.

Zhang et al. (2006) describe experiments comparing cluster analysis algorithms. They report that the Hopkins index is the most sensitive test for distinguishing fine scale clustering. They identify this fine scale resolution as particularly important in biological systems.

The Hopkins index has the advantage of being a generalized statistic that measures clusteredness rather than being specific to our experimental design.

Use of the Hopkins index requires the use of multiple datasets, with the Hopkins index computed for each. We generate 10 datasets for each configuration of targets and calculate a 95% confidence interval for the Hopkins statistic for each target configuration we test.

We use $m = 50$ sampling points and $n = 256$ targets. We repeat the analysis 100 times and report the mean Hopkins index in Figure 4. Since each configuration has 10 samples, there are 1000 Hopkins index samples contributing to each data point. This allows us to confirm that the empirical PDF is Gaussian distributed about the mean, which suggests that variation in the Hopkins index is due to random rather than systematic effects. We examine a total of 18 different distributions (10 linear and 8 power law progressions).

4.4 The Genetic Algorithm

We use a GA to find values of $\mathcal{H}$ that maximize search efficiency of the swarm for particular swarm sizes and Hopkins index. The objective function being optimized is the number of targets detected during a simulated search task. Optimization is potentially difficult because the objective function is probabilistic, computationally costly to evaluate, and non-differentiable. In addition, the optimization landscape is unknown and may be complex. In our previous work we have found GAs to be well suited to optimization tasks of this sort (Hecker and Moses, 2015).

The GA evaluates the fitness of various search strategies by simulating robots that search for targets. We vary the number of robots from 1 to 32 and the Hopkins index for target configurations from 0.5 to 1 and evolve $\mathcal{H}$ to maximize the search efficiency of the robot swarm. Fitness is defined as the number of targets detected by the robot swarm in one hour of simulated time. Because the fitness function is evaluated many times, the simulation must run quickly. Thus, we use a parsimonious simulation that uses a gridded, discrete world without explicitly modeling sensors or collision detection. This simple fitness function also helps to mitigate condition-specific idiosyncrasies and avoid over-fitted solutions (Hecker and Moses, 2015).

We evolve a population of 100 simulated robot swarms for 100 generations, though convergence consistently occurred in fewer generations. We used the recombination and mutation described in Hecker and Moses (2015). The GA evolves μ to determine $\mathcal{H}$ and to govern Equation (5). Parameter μ is randomly initialized using independent samples from the uniform distribution, $\mathcal{U}(1, 10)$, for each swarm. We allow μ to take on values above 3 in order to determine whether search patterns with extremely high intensity would evolve in the presence of error. Robots within a swarm use identical parameters throughout the hour-long experiment. During each generation, all 100 swarms undergo 8 fitness evaluations, each with different random placements drawn from the specified target distribution.

At the end of each generation, the fitness of each swarm is evaluated as the sum total of targets collected in the 8 runs. Deterministic tournament selection with replacement (tournament size = 2) is used to select 99 candidate swarm pairs. Each pair is recombined using uniform crossover and 10% Gaussian mutation with fixed standard deviation (0.05) to produce a new swarm population. We use elitism to copy the swarm with the highest fitness, unaltered, to the new population – the resulting 100 swarms make up the next generation. After only 10 to 20 generations, the evolutionary process converges on a $\mathcal{H}$ for the Lévy search.

4.5 Effect of the Number of Searchers and Target Configuration on $\mathcal{H}$

We use an Analysis Of Variance (ANOVA) (Hogg and Ledolter, 1987) to determine whether the relationships between factors (swarm size and the Hopkins index) and the observed $\mathcal{H}$ selected by the GA are statistically significant. The ANOVA also quantifies the relative contributions of factors to the resulting $\mathcal{H}$.

In Table 1 the error factor measures the amount of variation in evolved $\mathcal{H}$ that results from the combination of changes in the swarm size and number of target clusters. The sum of differences (SS) is used to calculate the Mean Squared Error (MSE), which measures the variance within and between factor groups.

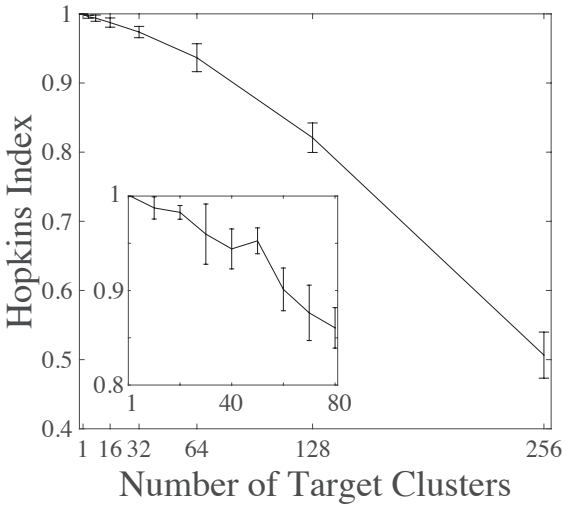

Figure 4: Hopkins index vs number of clusters. The Hopkins index is able to distinguish target configurations ranging from a single cluster to a uniform distribution of 256 singleton clusters on a scale of 0.5 to 1. Inset: Hopkins index for a linear progression of between 1 and 80 clusters.

5 Results

5.1 The Hopkins Statistic

We use the normalized Hopkins index as a measure of the clusteredness of target configurations in our experiments. The relationship between the number of clusters and the Hopkins index is given in Figure 4.

Following Zhang et al. (2006), we find that the Hopkins index is able to capture changes in target configuration over a wide range. However, the relationship between the number of clusters and the Hopkins index is non-linear, and it becomes more difficult to distinguish differences in target configurations as the number of clusters approaches 1. For example, the difference between 1 cluster and 40 clusters only maps to a 0.05 decrease in the Hopkins statistic. Despite this we are able to distinguish all 18 target configurations. We also find that the progression of target configurations, from 256 clusters of 1 target each

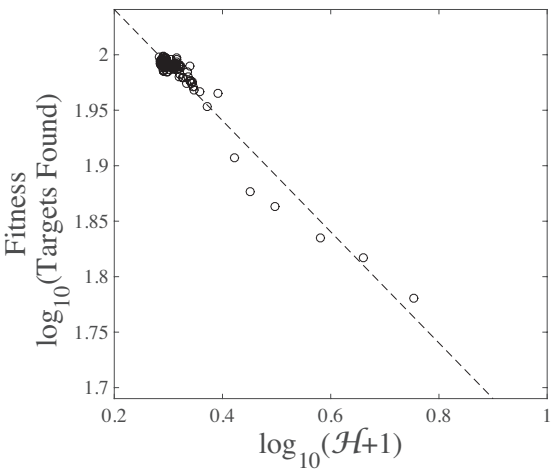

Figure 5: Convergence of the genetic algorithm on an optimum in the fitness landscape defined by $\mathcal{H}$. Fitness is defined to be the mean number of targets (open circles) detected in 1 h. The increase in fitness as the population approaches the optimal fractal dimension ($\mathcal{H}$) is fit well by a power law ($R^2 = 0.948$), indicated by the dashed line.

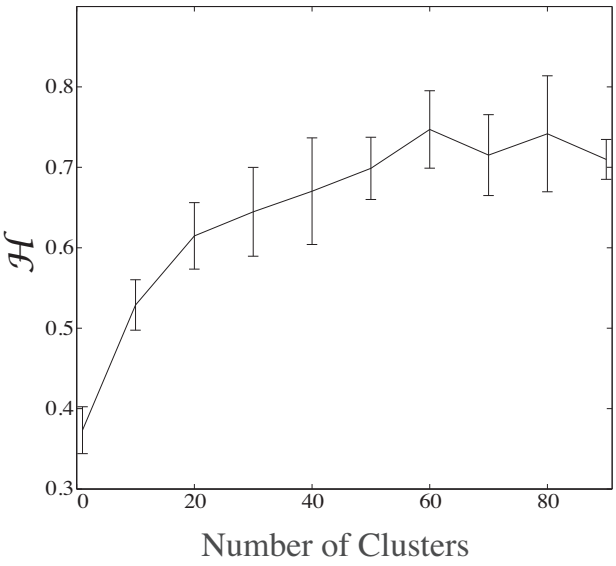

Figure 6: Dependence of evolved values of fractal dimension ($\mathcal{H}$) on target clusteredness. Bars indicate the 95% confidence interval (CI).

to 1 cluster of 256 targets, maps to the full range of the Hopkins index.

5.2 Fitness Landscape of the Fractal Search Dimension

We use the GA to explore the relationship between swarm size, the Hopkins index of the target configuration, and $\mathcal{H}$. The GA evolves values of $\mathcal{H}$ that provide a fitness advantage, where the fitness is the efficiency of target detection. We define efficiency to be the number of targets detected in one hour of search.

$\mathcal{H}$ is used as a measure of the trade-off between extent and intensity selected by the GA. The Hopkins index provides a metric for how disorganized the targets are.

An example evolution of $\mathcal{H}$ for 6 searchers and 100 clusters over 100 generations is visualized in Figure 5. The landscape has a clear slope from a randomly assigned starting value of $\mu = 6.3$ ($10^{0.8}$) to a peak at approximately 1.86 ($10^{0.27}$). A linear regression was performed and plotted on log-log transformed data (dashed line). The slope with 95% Confidence Interval (CI) is -0.501 ± 0.024 and intercept with 95% CI is 2.141 ± 0.008. ($R^2 = 0.948$, p-value $< 10^{-4}$). This suggests that the fitness landscape is steep, with a power law slope, and has a well defined optimum.

Figure 6 shows that the evolved $\mathcal{H}$ values are distinct for distributions of targets divided into 60 or fewer clusters. We note that below Hopkins index 0.9 the GA is unable to discover values of $\mathcal{H}$ that provide significant advantage over other values. The efficiency of Lévy search for distributions with Hopkins index between 0.75 and 0.9 are statistically similar and converge to $\mathcal{H} \approx 0.71$. For highly clustered distributions with Hopkins index between 0.9 and 1, $\mathcal{H}$ falls from 0.7 to ≈ 0.38 (Figure 7).

The rapid convergence of the GA in 10-25 generations to disjoint $\mathcal{H}$ depending on the factors defining the search environment, and the power law fitness

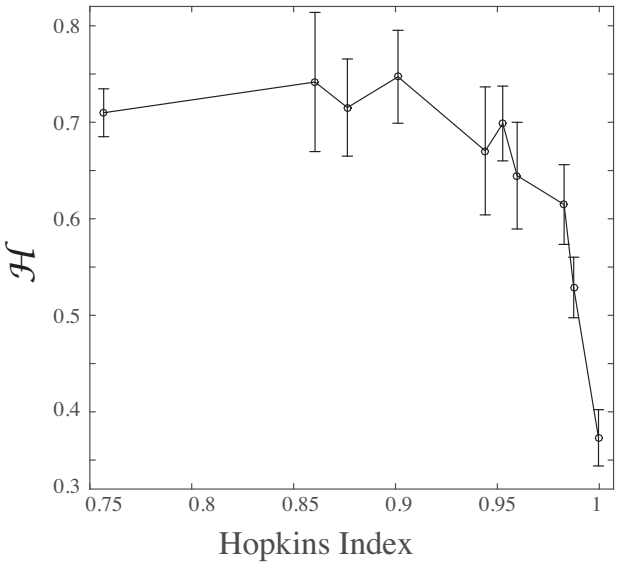

Figure 7: Dependence of evolved values of fractal dimension ($\mathcal{H}$) on the Hopkins index. Bars indicate the 95% confidence interval (CI).

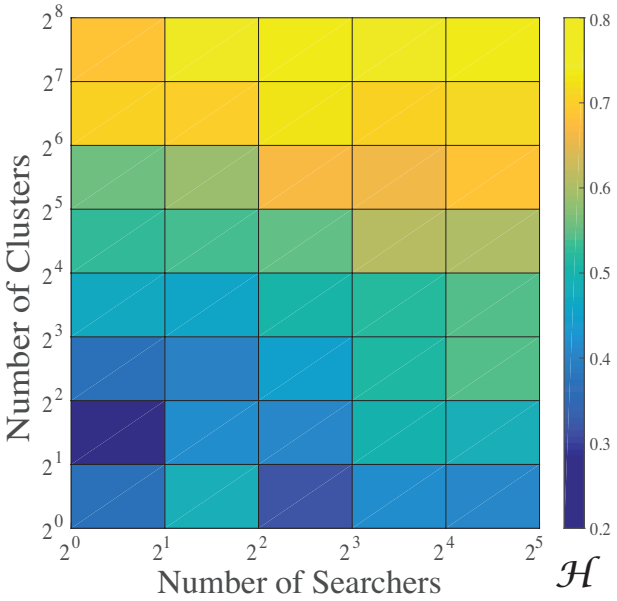

Figure 8: Full factorial heat map. Colors indicate GA-selected values of $\mathcal{H}$ for the specified swarm size and target configuration.

relationship as a function of $\mathcal{H}$ all indicate that the fitness landscape for $\mathcal{H}$ is easily optimized.

5.3 Optimizing Swarm Search

We used a full factorial experimental design to explore the relationship between $\mathcal{H}$ as selected by our GA, swarm size, and the configuration of targets. The results are displayed in Figure 8. For the target configuration closest to the uniform distribution (with Hopkins index = 0.5, 256 clusters), the optimal evolved $\mu = 1.8$ ($\mathcal{H} = 0.8$). This is close to the Viswanathan et al. (1999) prediction of an optimal μ of 2 ($\mathcal{H} = 1$) for the uniformly distributed target configuration.

A two-way ANOVA analysis shows a statistically significant correlation between the fractal dimension of the Lévy search evolved by the GA, swarm size, and the Hopkins index (Table 1). The p-values for the number of robots and the Hopkins index of target clustering are less than 10^{-5} and 10^{-18} respectively, indicating a statistically significant influence of swarm size and Hopkins index on values of $\mathcal{H}$.

Factor	SS	df	MSE	F	p-value
N Searchers	0.072	5	0.014	8.93	$< 10^{-4}$
Hopkins	0.682	8	0.085	53.15	$< 10^{-4}$
Error	0.064	40	0.002		
Total	0.818	53			

Table 1: ANOVA Results. The number of searchers and the Hopkins index both have statistically significant effects on the GA-selected $\mathcal{H}$. MSE is the remaining variance in $\mathcal{H}$ not explained by the factors.

The statistical tests indicate only that the GA selects different optimal values of $\mathcal{H}$ for different target configurations and varying numbers of searchers. We use simulations to measure how much search efficiency changes in response to different values of $\mathcal{H}$.

We create a multiple comparison plot (Montgomery, 2012) to further explore the relationships between the number of searchers, and $\mathcal{H}$ (Figure 9). The majority of fractal dimensions evolved for a particular cluster size in Figure 9a can be arranged into

(a) 8 Robots

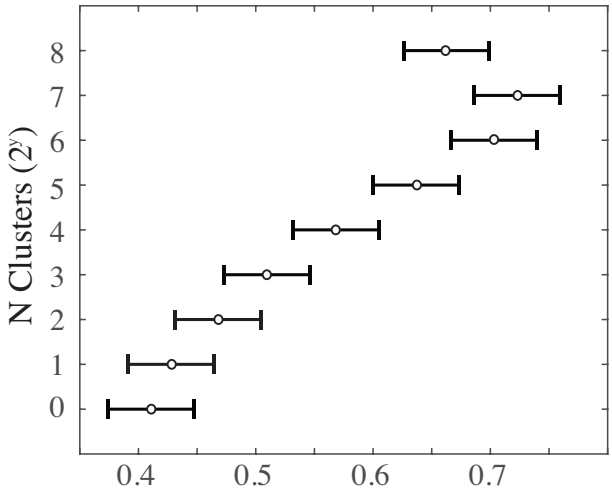

(b) Hopkins index = 0.85

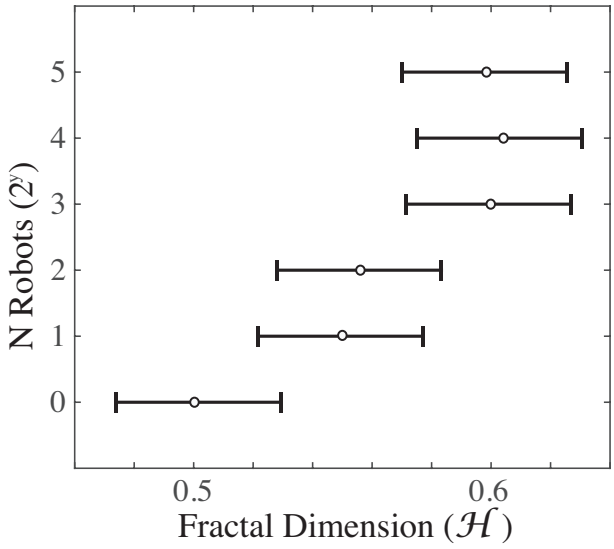

Figure 9: Multiple comparison plots showing the statistical separation of mean $\mathcal{H}$ grouped by the number of searchers and the number of clusters. In (a) most optimized values of $\mathcal{H}$ are statistically different from those evolved for a different target configuration. In (b) only $\mathcal{H}$ evolved for $N = 1$ is statistically different from $\mathcal{H}$ evolved for multiple robots. Open circles are sample means and the bars indicate the Tukey range test at 95% confidence. Non-overlapping bars indicate populations with means that are significantly different.

different statistically significant groups. However, Figure 9b shows that there is no statistical difference between fractal dimensions evolved for swarm sizes of $N > 1$.

In order to investigate the magnitude of the effect of $\mathcal{H}$ on search efficiency, we analyze four Lévy search patterns characterized by different $\mathcal{H}$ evolved for various numbers of searchers and for target configurations with different Hopkins indices.

Figures 10 shows the practical impact of the number of target clusters and the number of robots on efficiency. Each inter-quartile box is the result of 1000 searches. We plot the efficiency of a Brownian searcher for comparison.

In Figure 10(a) and (b), we evolve Lévy search patterns on different target configurations, 1 target cluster and 256 target clusters, while holding the number of robots fixed at 8. Lévy searchers perform much better when applied to the target configuration for which they were evolved than when applied to a target configuration for which they were not evolved. The change in median efficiency is 19% and 26%, with p-value $< 10^{-4}$ for both the Student's t-test and the Mann-Whitney U test.

In Figure 10(c) and (d), we repeat the experiment, but this time we hold the target configuration constant and vary the number of robots. Despite the statistically significant difference reported by the ANOVA, the change in efficiency is negligible. This suggests that the fitness landscape defined by the interaction of the number of searchers and $\mathcal{H}$ is relatively flat.

In summary, our results show that the configuration of targets, as measured by the Hopkins index of clusteredness, influences the $\mathcal{H}$ of optimal Lévy search. The dependence of the optimal $\mathcal{H}$ on the number of searchers (N) for $N > 1$ is not statistically significant. In all cases the practical impact of swarm size on search efficiency is minimal.

5.4 Efficiency Scaling with Number of Robots

When target discovery is difficult, for example when there is only a single cluster of targets (Hopkins index ≈ 1), the evolved $\mathcal{H}$ is approximately 0.4. In this

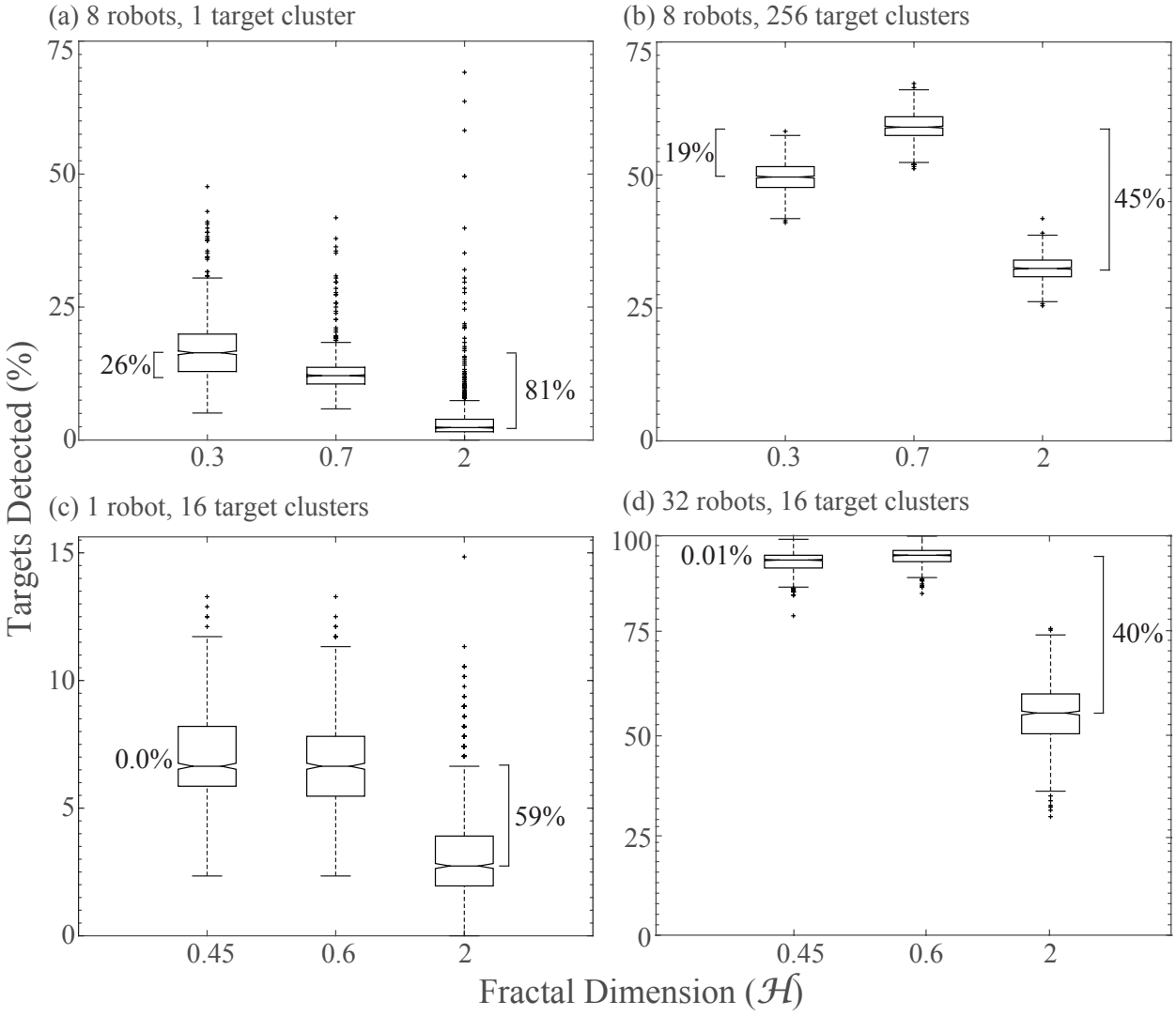

Figure 10: The effective efficiency of $\mathcal{H}$ depends strongly on the target configuration but not the swarm size. In (a) and (b) the search pattern with $\mathcal{H} = 0.7$ was evolved for a target configuration with Hopkins index = 0.5 (256 uniformly distributed targets). The search pattern with $\mathcal{H} = 0.3$ was evolved for Hopkins index = 0.99 (1 target cluster). As expected the difference in efficiency between Brownian search ($\mathcal{H} = 2$) and either Lévy search is large (45% and 81%). The mean efficiency gains for optimized values of $\mathcal{H}$ are large (19% and 26%). In (c) and (d) the search pattern with $\mathcal{H} = 0.6$ was evolved for a swarm with 32 robots. The search pattern with $\mathcal{H} = 0.45$ was evolved for a swarm with 1 robot. The difference in efficiency between Brownian search and either Lévy search is large (40% and 59%). The percentage change between the mean number of targets discovered by the search pattern evolved for 1 and 32 robots is small (0.0% and 0.01%).

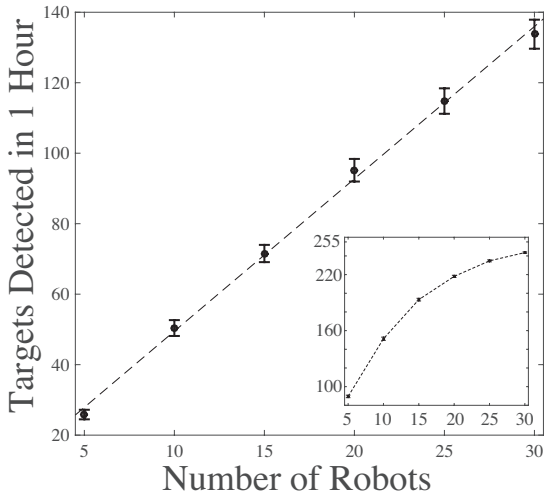

Figure 11: Search efficiency scales linearly with the number of robots. Closed circles are mean values and bars are the 95% confidence interval for 100 samples. Targets are clustered with Hopkins index ≈ 1.0 (1 cluster). The dashed line is the linear regression ($R^2 = 0.924$, p-value $< 5 \times 10^{-3}$). Inset: 64 clusters (Hopkins index = 0.93). The search space saturates resulting in sublinear scaling. Circles are mean values and bars are the 95% confidence interval for 100 samples. The dashed line is a linear interpolation.

case the relationship between the number of searchers and search efficiency is linear (Figure 11). Doubling the number of robots doubles the number of detected targets. This scalability is in contrast with studies of other movement patterns, where per robot search efficiency declines with number of searchers (Winfield et al., 2005; Hecker and Moses, 2015).

However, we note that linear scaling does not hold in all cases. Over time the searched area becomes saturated with unsearched locations becoming increasingly hard to find (Stone, 1975). This effect is seen in the Figure 11 inset, where we see saturation after more than half the targets are collected. When the target configuration is more uniform, targets are depleted quickly and the effect of saturation results in sublinear scaling. Targets with higher Hopkins index allow search efficiency to scale with the number of searchers since saturation is negligible.

6 Discussion

When robots are prone to malfunction, have imperfect sensors, or must work in natural environments, stochastic search provides a useful alternative strategy to deterministic search. Harris et al. (2012) found that T cells searching in peripheral tissue can be modeled using a Lévy search. In previous work we observed the stochastic search patterns of T cells searching for dendritic cells in lymph nodes and characterized them as being reasonably approximated by a heavy-tailed search pattern (Fricke et al., 2013, 2016). Here we explore the ability to optimize the efficiency of Lévy search in a robot swarm.

A significant advantage of Lévy search is its simplicity and adaptability: a range of search behaviors can be defined using just one parameter. Evolving solutions is fast since the fitness landscapes are simple with well defined optima (Figure 5).

Our analysis shows that there is a systematic relationship between the Hausdorff Fractal Dimension ($\mathcal{H}$) optimized by a Genetic Algorithm (GA), the number of searchers, and the configuration of targets as measured by the Hopkins index. Specifically, $\mathcal{H}$ selected by the GA decreases as the clusteredness and the Hopkins index of the targets increase. This supports a prediction made by (Raposo et al., 2011) based on their theoretical analysis of the one-dimensional case.

Using this empirical relationship (Figure 8) we are able to predict values of $\mathcal{H}$ that result in improved search performance given various target configurations. The GA revealed a simple fitness landscape that likely could be explored with other optimization methods.

The fractal dimension of Lévy search can easily be adapted to the configuration of targets (Figure 10). In future work we will leverage this property to allow robot swarms capable of online classification of target distributions to select the value of $\mathcal{H}$ that results in the most efficient search strategy.

While an ANOVA shows that the number of searchers has a statistically significant effect on the GA-selected value of $\mathcal{H}$, this translates into negligible differences in search efficiency (Figure 10 panels (c) and (d)). We also find a linear relationship between the number of searchers and the efficiency of search, up to the point where so many targets have been found that search itself becomes more difficult (Figure 11). The insensitivity of Lévy search efficiency to the number of searchers is a clear benefit to swarm robotics. As robots fail or get lost, the optimal $\mathcal{H}$ for a given target configuration does not change substantially.

A possible explanation for the linear scale-up in efficiency with the number of Lévy, as opposed to Brownian, searchers, is that when Brownian searchers start from the same location the high fractal dimension of their movement results in locations being revisited by other robots in the swarm. For n searchers the number of unique locations visited in time t is proportional to $t \ln\left(\frac{n}{\ln t}\right)$. Only after t exceeds e^n do searchers employing Brownian search avoid oversampling (Larralde et al., 1992). For a swarm of 256 robots performing Brownian search this implies wasted effort for more than 10^{100} time steps. In contrast, for n searchers employing an evolved Lévy search pattern, the number of unique locations visited is proportional to nt, resulting in relatively little oversampling (Viswanathan et al., 1996).

We also find that there is little interaction between the number of searchers and the configuration of targets; the lack of interaction in those factors removes a potential complication in the proper selection of $\mathcal{H}$.

Lévy search has been used to model biological search including immunological search. The properties of Lévy search we explore in this paper have implications for the biological systems in which Lévy search models have been suggested. For example, in the immune system T cell swarms of various sizes are required to find a wide variety of targets distributed in different ways in different tissues. The distribution of dendritic cell targets in lymph nodes may be very different than virus-infected cells in the lung or brain, and in each case the number and distribution of targets may change over time. Because targets of immunological search are heterogeneously distributed, and the number of searchers vary by many orders of magnitude during the search process, the adaptability and scalability of Lévy search may be particularly useful in immune search. Our adaptation of the Lévy exponent with a GA suggests how a simple movement pattern could be adapted by natural selection to search efficiently given a variety of target configurations over a wide range of T cell numbers.

Search for clustered targets is an important problem in swarm robotics because it generalizes to many real-world applications, such as collecting hazardous materials, natural resources, search and rescue, and environmental monitoring (Liu et al., 2007; Parker, 2009; Winfield, 2009; Brambilla et al., 2013). A particularly exciting application is space exploration. For example, NASA recently announced the Swarmathon challenge in which robots operate in concert to autonomously search for, retrieve, and map patchy natural resources, such as water ice. These robot swarms are intended to be used for resource exploration on other planets (Ramsey, 2015). In this arena particularly, robot searchers must be robust to hardware failure and sensor limitations, and adaptable to heterogeneous target configurations. Scalability is desirable because it allows flexibility in robot allocation. For example, rich resource areas may be assigned more robots without loss of efficiency. Our work demonstrates a mechanism for tuning the fractal dimension of a search pattern to most efficiently encounter targets given a measure of their clusteredness, while also being scalable and robust.

References

Acar, E. U., Choset, H., Zhang, Y., and Schervish, M. (2003). Path planning for robotic demining: Robust sensor-based coverage of unstructured environments and probabilistic methods. *The International Journal of Robotics Research*, 22(7-8):441–466.

Ackley, D. H., Cannon, D. C., and Williams, L. R. (2012). A movable architecture for robust spatial computing. *The Computer Journal*, page bxs129.

Alberts, B., Johnson, A., Lewis, J., Raff, M., Roberts, K., and Walter, P. (2002). *Molecular Bi-*

ology of the Cell. Garland Science, New York, 4th edition.

Ariotti, S., Beltman, J. B., Chodaczek, G., Hoekstra, M. E., van Beek, A. E., Gomez-Eerland, R., Ritsma, L., van Rheenen, J., Marée, A. F. M., and Zal, T. (2012). Tissue-resident memory CD8+ T cells continuously patrol skin epithelia to quickly recognize local antigen. *Proceedings of the National Academy of Sciences*, 109(48):19739–19744.

Banerjee, S., Levin, D., Moses, M., Koster, F., and Forrest, S. (2011). The value of inflammatory signals in adaptive immune responses. In *Artificial Immune Systems*, pages 1–14. Springer.

Banigan, E. J., Harris, T. H., Christian, D. A., Hunter, C. A., Liu, A. J., and Asquith, B. (2015). Heterogeneous CD8+ T Cell Migration in the Lymph Node in the Absence of Inflammation Revealed by Quantitative Migration Analysis. *PLoS computational biology*, 11(2):e1004058–e1004058.

Bartumeus, F., da Luz, M. G. E., Viswanathan, G. M., and Catalan, J. (2005). Animal search strategies: a quantitative random-walk analysis. *Ecology*, 86(11):3078–3087.

Beal, J. (2015). Superdiffusive Dispersion and Mixing of Swarms. *ACM Transactions on Autonomous and Adaptive Systems (TAAS)*, 10(2):10.

Bénichou, O., Loverdo, C., Moreau, M., and Voituriez, R. (2011). Intermittent search strategies. *Reviews of Modern Physics*, 83(1):81.

Birk, A. and Carpin, S. (2006). Rescue robotics - a crucial milestone on the road to autonomous systems. *Advanced Robotics*, 20(5):595–605.

Brambilla, M., Ferrante, E., Birattari, M., and Dorigo, M. (2013). Swarm robotics: a review from the swarm engineering perspective. *Swarm Intelligence*, 7(1):1–41.

Celli, S., Day, M., Müller, A. J., Molina-Paris, C., Lythe, G., and Bousso, P. (2012). How many dendritic cells are required to initiate a T-cell response? *Blood*, 120(19):3945–3948.

De Boer, R. J., Oprea, M., Antia, R., Murali-Krishna, K., Ahmed, R., and Perelson, A. S. (2001). Recruitment times, proliferation, and apoptosis rates during the CD8+ T-cell response to lymphocytic choriomeningitis virus. *Journal of virology*, 75(22):10663–10669.

Donovan, G. M. and Lythe, G. (2012). T-cell movement on the reticular network. *Journal of theoretical biology*, 295:59–67.

Edwards, A. M. (2011). Overturning conclusions of Lévy flight movement patterns by fishing boats and foraging animals. *Ecology*, 92(6):1247–1257.

Fink, W., Dohm, J. M., Tarbell, M. A., Hare, T. M., and Baker, V. R. (2005). Next-generation robotic planetary reconnaissance missions: a paradigm shift. *Planetary and Space Science*, 53(14):1419–1426.

Fricke, G. M., Asperti-Boursin, F., Hecker, J., Cannon, J., and Moses, M. (2013). From Microbiology to Microcontrollers: Robot Search Patterns Inspired by T Cell Movement. In *Advances in Artificial Life, ECAL*, volume 12, pages 1009–1016.

Fricke, G. M., Letendre, K. A., Moses, M. E., and Cannon, J. L. (2016). Persistence and Adaptation in Immunity: T Cells Balance the Extent and Thoroughness of Search. *PLoS Comput Biol*, 12(3):e1004818.

Fricke, G. M. and Thomas, J. L. (2006). Receptor aggregation by intermembrane interactions: A Monte Carlo study. *Biophysical Chemistry*, 119(2):205–211.

Gérard, A., Patino-Lopez, G., Beemiller, P., Nambiar, R., Ben-Aissa, K., Liu, Y., Totah, F. J., Tyska, M. J., Shaw, S., and Krummel, M. F. (2014). Detection of Rare Antigen-Presenting Cells through T Cell-Intrinsic Meandering Motility, Mediated by Myo1g. *Cell*, 158(3):492–505.

Groom, J. R., Richmond, J., Murooka, T. T., Sorensen, E. W., Sung, J. H., Bankert, K., von Andrian, U. H., Moon, J. J., Mempel, T. R., and Luster, A. D. (2012). CXCR3 chemokine receptor-ligand interactions in the lymph node optimize CD4+ T helper 1 cell differentiation. *Immunity*, 37(6):1091–1103.

Harris, T. H., Banigan, E. J., Christian, D. A., Konradt, C., Wojno, E. D. T., Norose, K., Wilson, E. H., John, B., Weninger, W., Luster, A. D., and

Others (2012). Generalized Lévy walks and the role of chemokines in migration of effector CD8+ T cells. *Nature*, 486(7404):545–548.

Hecker, J. P. and Moses, M. E. (2015). Beyond pheromones: evolving error-tolerant, flexible, and scalable ant-inspired robot swarms. *Swarm Intelligence*, 9(1):43–70.

Hecker, J. P., Stolleis, K., Swenson, B., Letendre, K., and Moses, M. E. (2013). Evolving Error Tolerance in Biologically-Inspired iAnt Robots. In *Proceedings of the Twelfth European Conference on the Synthesis and Simulation of Living Systems (Advances in Artificial Life, ECAL 2013)*, pages 1025–1032.

Hogg, R. V. and Ledolter, J. (1987). *Engineering statistics*. Macmillan Pub Co.

Hu, H., Oyekan, J., and Gu, D. (2011). A school of robotic fish for pollution detection in port. *Biologically Inspired Robotics (Y. Liu and D. Sun, eds.)*, pages 85–104.

Hughes, B. D. (1996). *Random walks and random environments*. Clarendon Press Oxford.

Humphreys, T. E., Ledvina, B. M., Psiaki, M. L., O'Hanlon, B. W., and Kintner Jr, P. M. (2008). Assessing the spoofing threat: Development of a portable GPS civilian spoofer. In *Proceedings of the ION GNSS international technical meeting of the satellite division*, volume 55, page 56.

Humphries, N. E., Weimerskirch, H., Queiroz, N., Southall, E. J., and Sims, D. W. (2012). Foraging success of biological Lévy flights recorded in situ. *Proceedings of the National Academy of Sciences*, 109(19):7169–7174.

Jain, A. K. and Dubes, R. C. (1988). *Algorithms for clustering data*, volume 6. Prentice hall Englewood Cliffs.

James, A., Plank, M. J., and Edwards, A. M. (2011). Assessing Lévy walks as models of animal foraging. *Journal of The Royal Society Interface*, 8(62):1233–1247.

Katada, Y., Nishiguchi, A., Moriwaki, K., and Watakabe, R. (2015). Swarm Robotic Network Using Lévy Flight in Target Detection Problem. In *Proceedings of The First International Symposium on Swarm Behavior and Bio-Inspired Robotics (SWARM2015)*, pages 310–315.

Keeter, M., Moore, D., Muller, R., Nieters, E., Flenner, J., Martonosi, S. E., Bertozzi, A. L., Percus, A. G., and Levy, R. (2012). Cooperative search with autonomous vehicles in a 3d aquatic testbed. In *American Control Conference (ACC), 2012*, pages 3154–3160. IEEE.

Larralde, H., Trunfio, P., Havlin, S., Stanley, H. E., and Weiss, G. H. (1992). Territory covered by N diffusing particles. *Nature*, 355(6359):423–426.

Linderman, J. J., Riggs, T., Pande, M., Miller, M., Marino, S., and Kirschner, D. E. (2010). Characterizing the dynamics of CD4+ T cell priming within a lymph node. *The Journal of Immunology*, 184(6):2873–2885.

Lindquist, R. L., Shakhar, G., Dudziak, D., Wardemann, H., Eisenreich, T., Dustin, M. L., and Nussenzweig, M. C. (2004). Visualizing dendritic cell networks in vivo. *Nature immunology*, 5(12):1243–1250.

Liu, W., Winfield, A. F. T., and Sa, J. (2007). Modelling swarm robotic systems: A case study in collective foraging. *Towards autonomous robotic systems (TAROS 07)*, pages 25–32.

Love, J., Amai, W., Blada, T., Little, C., Neely, J., and Buerger, S. (2015). The Sandia architecture for heterogeneous unmanned system control (SAHUC). In *Proc. SPIE 9464, Ground/Air Multisensor Interoperability, Integration, and Networking for Persistent ISR VI*. International Society for Optics and Photonics.

Maier, D. and Kleiner, A. (2010). Improved GPS sensor model for mobile robots in urban terrain. In *Robotics and Automation (ICRA), 2010 IEEE International Conference on*, pages 4385–4390. IEEE.

Mandelbrot, B. B. (1983). *The fractal geometry of nature*, volume 173. Macmillan.

Mårell, A., Ball, J. P., and Hofgaard, A. (2002). Foraging and movement paths of female reindeer: insights from fractal analysis, correlated random

walks, and Lévy flights. *Canadian Journal of Zoology*, 80(5):854–865.

Méndez, V., Campos, D., and Bartumeus, F. (2013). *Stochastic foundations in movement ecology: anomalous diffusion, front propagation and random searches*. Springer Science & Business Media.

Miller, M. J., Hejazi, A. S., Wei, S. H., Cahalan, M. D., and Parker, I. (2004). T cell repertoire scanning is promoted by dynamic dendritic cell behavior and random T cell motility in the lymph node. *Proceedings of the National Academy of Sciences of the United States of America*, 101(4):998–1003.

Mirsky, H. P., Miller, M. J., Linderman, J. J., and Kirschner, D. E. (2011). Systems biology approaches for understanding cellular mechanisms of immunity in lymph nodes during infection. *Journal of theoretical biology*, 287:160–170.

Montgomery, D. C. (2012). *Design and analysis of experiments*. John Wiley & Sons, 8th edition.

Nurzaman, S. G., Matsumoto, Y., Nakamura, Y., Koizumi, S., and Ishiguro, H. (2009). Yuragi-based adaptive searching behavior in mobile robot: From bacterial chemotaxis to Lévy walk. In *Robotics and Biomimetics, 2008. ROBIO 2008. IEEE International Conference on*, pages 806–811. IEEE.

Nurzaman, S. G., Matsumoto, Y., Nakamura, Y., Shirai, K., Koizumi, S., and Ishiguro, H. (2011). From Levy to Brownian: A computational model based on biological fluctuation. *PloS one*, 6(2):e16168.

Parker, L. E. (2009). Path planning and motion coordination in multiple mobile robot teams. *Encyclopedia of complexity and system science*, pages 5783–5800.

Potdar, A. A., Jeon, J., Weaver, A. M., and Cummings, P. T. (2008). Cell Migration Paths of Epithelial Cells Resemble Lévy Modulated Correlated Random Walk Pattern. In *Proceedings of the 2008 Annual Meeting of the American Institute of Chemical Engineers*.

Raichlen, D. A., Wood, B. M., Gordon, A. D., Mabulla, A. Z. P., Marlowe, F. W., and Pontzer, H. (2014). Evidence of Lévy walk foraging patterns in human huntergatherers. *Proceedings of the National Academy of Sciences*, 111(2):728–733.

Ramsey, S. (2015). NASA Awards Grant to Manage Swarmathon Challenge (press release).

Raposo, E. P., Bartumeus, F., Da Luz, M. G. E., Ribeiro-Neto, P. J., Souza, T. A., and Viswanathan, G. M. (2011). How landscape heterogeneity frames optimal diffusivity in searching processes. *PLoS computational biology*, 7(11):e1002233.

Sahin, E. (2005). Swarm robotics: From sources of inspiration to domains of application. In *Swarm robotics*, pages 10–20. Springer.

Seshadri, V. and West, B. J. (1982). Fractal dimensionality of Lévy processes. *Proceedings of the National Academy of Sciences of the United States of America*, 79(14):4501.

Shlesinger, M. F. and Klafter, J. (1986). Lévy walks versus Lévy flights. In *On growth and form*, pages 279–283. Springer.

Stephens, D. W. and Krebs, J. R. (1986). *Foraging theory*. Princeton University Press.

Stolleis, K. A., Hecker, J. P., Montague, G., Leucht, K., and Moses, M. E. (2016a). Evolving Autonomous Charging Behavior in a Robot Swarm. In *Proceedings of Earth & Space 2016 Engineering for Extreme Environments*.

Stolleis, K. A., Hecker, J. P., and Moses, M. E. (2016b). The Ant and the Trap: Evolution of Ant-Inspired Obstacle Avoidance in a Multi-Agent System. In *Proceedings of Earth & Space 2016 Engineering for Extreme Environments*.

Stone, L. D. (1975). *Theory of optimal search*. Academic Press New York.

Sung, J. H., Zhang, H., Moseman, E. A., Alvarez, D., Iannacone, M., Henrickson, S. E., Juan, C., Groom, J. R., Luster, A. D., and von Andrian, U. H. (2012). Chemokine guidance of central memory T cells is critical for antiviral recall responses in lymph nodes. *Cell*, 150(6):1249–1263.

Sutantyo, D., Levi, P., Moslinger, C., and Read, M. (2013). Collective-adaptive lévy flight for underwater multi-robot exploration. In *Mechatron-*

ics and Automation (ICMA), 2013 IEEE International Conference on, pages 456–462. IEEE.

Sutantyo, D. K., Kernbach, S., Levi, P., and Nepomnyashchikh, V. A. (2010). Multi-Robot searching algorithm using Lévy flight and artificial potential field. In *Safety Security and Rescue Robotics (SSRR), 2010 IEEE International Workshop on*, pages 1–6. IEEE.

Tamura, K. and Naruse, K. (2014). Unsmooth field sweeping by Balistic random walk of multiple robots in unsmooth terrain. In *Soft Computing and Intelligent Systems (SCIS), 2014 Joint 7th International Conference on and Advanced Intelligent Systems (ISIS), 15th International Symposium on*, pages 585–589. IEEE.

Taylor, L. R. (1961). Aggregation, variance and the mean. *Nature*, pages 732–735.

Textor, J., Henrickson, S. E., Mandl, J. N., von Andrian, U. H., Westermann, J., de Boer, R. J., and Beltman, J. B. (2014). Random migration and signal integration promote rapid and robust T cell recruitment. *PLoS computational biology*, 10(8):e1003752.

United States Department of Defense (2008). Global positioning system standard positioning service performance standard. *SPSGPS*, 4th Ed.:9–15.

Van Dartel, M., Postma, E., van den Herik, J., and de Croon, G. (2004). Macroscopic analysis of robot foraging behaviour. *Connection Science*, 16(3):169–181.

Viswanathan, G. M., Afanasyev, V., Buldyrev, S. V., Murphy, E. J., Prince, P. A., and Stanley, H. E. (1996). Lévy flight search patterns of wandering albatrosses. *Nature*, 381(6581):413–415.

Viswanathan, G. M., Buldyrev, S. V., Havlin, S., Da Luz, M. G. E., Raposo, E. P., and Stanley, H. E. (1999). Optimizing the success of random searches. *Nature*, 401(6756):911–914.

Von Neumann, J. (1951). The general and logical theory of automata. *Cerebral mechanisms in behavior*, 1:1–41.

Weber, T. R. (1995). An Analysis of Lemmings: A Swarming Approach to Mine Countermeasures in the VSW/SZ/BZ. Technical report, DTIC Document.

Winfield, A. F. T. (2009). Foraging Robots. In Meyers, R. A., editor, *Encyclopedia of complexity and systems science*, pages 3682–3700. Springer, New York.

Winfield, A. F. T., Harper, C. J., and Nembrini, J. (2005). Towards dependable swarms and a new discipline of swarm engineering. In *Swarm robotics*, pages 126–142. Springer.

Zhang, J., Leiderman, K., Pfeiffer, J. R., Wilson, B. S., Oliver, J. M., and Steinberg, S. L. (2006). Characterizing the topography of membrane receptors and signaling molecules from spatial patterns obtained using nanometer-scale electron-dense probes and electron microscopy. *Micron*, 37(1):14–34.

7 Acknowledgements

The authors gratefully acknowledge financial support from NASA NSR681787 (GMF, MM), NSF EF 1038682 (MM), DARPA P-1070-113237 (MM), NIH 1R01AI097202 (JLC), the Spatiotemporal Modeling Center 1 P50 GM085273 (JLC), the Center for Evolution and Theoretical Immunology 5P20GM103452 (JLC), and a James S. McDonnell Foundation grant for the study of Complex Systems (MM). We also thank the reviewers, each of whom provided insightful comments and corrections that have greatly improved this manuscript.

8 Conflicts of Interest

9 Notes

For more information about the iAnt platform including instructions on how to build them visit: http://swarms.cs.unm.edu